Research Paper

Bending of Beams with Symmetrically Varying Mechanical Properties Under Generalized Load – Shear effect

Krzysztof MAGNUCKI, Jerzy LEWINSKI*

Institute of Rail Vehicles TABOR
Warszawska 181, 61-055 Poznan, Poland
*Corresponding Author e-mail: jerzy.lewinski@tabor.com.pl

The paper is devoted to simply supported beams with symmetrically varying mechanical properties in the depth direction. Generalized load of the beams includes the load types from uniformly distributed to point load (three-point bending). This load is analytically described with the use of a certain function including a dimensionless parameter. The value of the parameter is decisive for the load type. The individual nonlinear "polynomial" hypothesis is applied to deformation of a planar cross section. Based on the definitions of the bending moment and the shear transverse force the differential equation of equilibrium is obtained. The equation is analytically solved and the deflections are calculated for an exemplary beam family. The results of the study are specified in tables.

Key words: FGM beams; bending; analytical modeling.

1. INTRODUCTION

Contemporary studies related to bending, buckling and vibrations of the beams, plates and shells made of Functionally Graded Materials (FGM) are intensively developed. The shear effect in these structures is significant. The problem is presented in details in the following papers.

WANG *et al.* [1] presented the theories of beams and plates developed in the 20th century with consideration of the shear effect. In the works devoted to this subject only the classical Euler-Bernoulli/Kirchhoff theory is applied. Meanwhile, such an approach is inadequate in case of deep beams and thick plates where the effect of transverse shear strains becomes significant. The authors demonstrate that the shear deformation theories improve the solutions as compared to the classical theory. MAGNUCKI and STASIEWICZ [2] dealt with elastic buckling of a beam of rectangular cross-section, made of an isotropic porous material. The beam is simply supported at both ends and subjected to lengthwise compressive force. The properties of the porous material vary with respect

to the beam thickness. The differential equations governing the beam stability are derived based on the principle of stationarity of the total potential energy and solved analytically. The solution provides an explicit expression for critical load of the compressed beam. The results are confirmed by the Finite Element Method computation. MAGNUCKA-BLANDZI [3] solved the problem of buckling and deflection of a circular porous-cellular plate simply supported at its edge. The plate was subjected to radial uniform compression and uniform pressure. Mechanical properties of the plate porous material vary with respect to its thickness. Based on the principle of stationarity of the total potential energy a system of differential equations was derived that allowed to determine the critical load and deflection. THAI and VO [4] developed several higher-order theories taking into account the shear effect arising while bending and free vibration of functionally graded beams. To a certain extent these theories were similar to the Euler-Bernoulli beam theory as they resulted in comparable equations of motion and boundary conditions derived from the Hamilton's principle, as well as the stress resultant expressions. The authors presented analytical solutions and compared their results to the existing ones with a view to verify the suitability of the theories. DEHROUYEH-SEMNANI and BAHRAMI [5] developed two size-dependent Timoshenko beam finite elements based on the modified couple stress theory – of four and six degrees of freedom (dof). The authors examined usefulness of these elements in solving the beam static bending. It was proved that the results computed with the 6-dof element perfectly agree with the ones obtained from other model calculations. MAGNUCKI *et al.* [6] studied three-point bending of a short beam. The values of elastic modules varied in respect to thickness of the beam. Three differential equations of the beam equilibrium were obtained based on the principle of stationary potential energy. Distribution of the shear stresses arising in cross section of the beam as well as the deflections were determined. A numerical – FEM model of the beam was developed with a view to verify the analytical results. PACZOS *et al.* [7] studied a short sandwich beam of special honeycomb structure of the core. Values of elastic modules of the beam material vary with respect to its length. Analytical model of the beam is based on the "zigzag" hypothesis of planar cross section deformation. Deflection of the beam is calculated analytically and experimentally determined. Both results are compared with each other.

Particular group of the papers enumerated below is devoted to the structures made of functionally graded materials (FGM).

SANKAR [8] studied a functionally graded beam subjected to transverse loads, in which the Young's modulus exponentially varies with respect to the beam thickness. This exponential variation enabled to define a single non-dimensional parameter controlling the Young's modulus values. A simple Euler-Bernoulli type beam model was adopted. It was found that such an assumption is effective only

for long and slender beams. KADOLI *et al.* [9] focused on static behaviour of functionally graded beams composed of metal and ceramic materials with varying metal to ceramic ratio. The static equilibrium equation of the beam of finite element form was formulated based on the principle of stationary potential energy. The authors presented a comprehensive discussion of the numerical results obtained for the case of relatively thick beam subjected to uniformly distributed load and various boundary conditions. KAPURIA *et al.* [10] devoted their paper to theoretical and experimental analysis of layered functionally graded beams. They studied bending and free vibration of the beams using the third order zigzag theory with a view to determine the effective modules of elasticity of particular layers. Theoretical predictions calculated for the beams with varying ceramic content are compared to the experiment results. The zigzag theory proved to be an effective tool for modelling of these beams. GIUNTA *et al.* [11] analyzed the beams made of functionally graded materials using classical and more sophisticated theories. The authors proposed several theories enabling analysis of the beams made of the materials the properties of which vary along one or two directions. The classical beam theories are then particular cases of these new theories. Various beam height to length ratios were considered. The results obtained analytically were verified by three-dimensional finite element models. KAHROBAIYAN *et al.* [12] formulated a new model of functionally graded Euler-Bernoulli beam. The model considered the size-effect in micro-scale and, therefore, was composed of functionally graded microbeams. The governing equation and boundary conditions were obtained using a variational method. The problems of static bending and free-vibration of the model are considered for the microbeams, the material properties of which varied with respect to thickness in accordance with power law. The results were compared to the ones obtained with the help of classical continuum theories. LI *et al.* [13] presented the bending problems of the Timoshenko beams made of functionally graded materials (FGM). The governing equations are analytically derived using the Euler-Bernoulli theory for homogenous beams. The bending moment, shear force, deflection and rotational angle of the beam are expressed in terms of deflection of a homogenous Euler-Bernoulli beam with the same geometry, load and end constraints. The analytical solutions obtained this way may serve as guidelines for further research of FGM beams. ZHANG [14] studied bending of the functionally graded beams using the physical neutral surface theory and adopting nonlinear von Kármán strain-displacement relationships. The author assumed that the material properties depend on temperature and vary with respect to beam thickness. The approximate solutions of the beam bending problem were obtained using the Ritz method. RAHAEIFARD *et al.* [15] applied the strain gradient theory to analysis of the nonlinear Euler-Bernoulli beams made of functionally graded materials. Composition of the beam material varies with respect to beam thickness based on a power law. The non-

linear governing equation and boundary conditions were determined with the use of the Hamilton's principle. Static deflection and free vibration of the beam were computed. The calculations have shown that the classical theories may be considered as special cases of the strain gradient theory. CHEN et al. [16] presented the solutions of elastic buckling and static bending of shear deformable functionally graded porous beams, using the Timoshenko beam theory. A system of differential equation governing behaviour of the porous beams was obtained with the use of the Hamilton's principle. It was found that variation of the porosity distribution affects the structural performance that enabled to suggest the porosity pattern ensuring better buckling resistance and bending behaviour. LI and HU [17] used the nonlocal strain gradient theory to study the nonlinear bending and free vibrations of two-constituent functionally graded beams. The authors adopted the nonlinear Euler-Bernoulli and Timoshenko beam models and, based on the Hamilton's principle, formulated the equations of motion and boundary conditions. The stretching effect of the beam mid-plane caused that the nonlinear bending deflections were smaller as compared to linear cases subjected to the same force, while the nonlinear vibration frequencies exceeded the ones obtained with the use of linear approach. NEJAD and HADI [18] devoted their work to the problem of static bending of Euler-Bernoulli nano-beams made of a functionally graded material. Material properties of the beam, being an Euler-Bernoulli nano-beam, vary with respect to thickness and length, according to arbitrarily chosen function. The model of the beam is formulated with the use of the Eringen's nonlocal elasticity theory. The governing equations are formulated based on the principle of minimum potential energy. Several numerical results are presented, showing the effects of the pattern of material properties variability on bending.

SAYYAD and GHUGAL [19] provided a review of the literature devoted to bending, buckling and free vibration of the composite and sandwich beams. The authors specify many literature items dealing with shear deformable isotropic, laminated composite and sandwich beams, using various theories. The review cites 515 references, suggests possible scope of further research on the subject. MAGNUCKI et al. [20] presented a work devoted to bending and free vibration of porous beams with consideration of the shear effect. Mechanical properties of the beam change with respect to its thickness, symmetrically with regard to the neutral axis. The functions adjusting the pattern of the material variability are so formulated as to reflect homogeneous, nonlinearly variable and sandwich structures. The Hamilton's principle allowed to derive two differential equations of motion that are solved analytically. TAATI [21] presented an accurate solution of buckling and post-buckling behaviour of functionally graded micro-beams under combined thermomechanical loads. The equations governing these phenomena have been derived based on the principle of minimum total potential energy, using the modified couple stress theory. Exact solution of the equations was ob-

tained by the differential operator method. Moreover, a detailed discussion of the effects of geometry, and material distribution variation on the post-buckling behaviour is presented.

The subject of the study are simply supported beams of length L, width b, and depth h with symmetrically varying mechanical properties in the depth direction. The bending problem of the beams is analytically studied, with consideration of the shear effect. The beams carry the generalized transverse load of intensity $q(x)$ (Fig. 1).
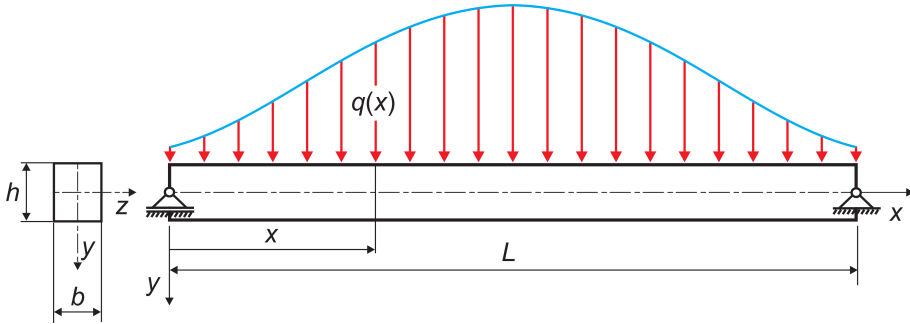
FIG. 1. Scheme of the simply supported beam with the generalized transverse load.

The paper includes an original formulation of the load, allowing to define the load distribution from the uniform one to a concentrated force. The study is focused on a family of the beams subjected to some selected load cases.

2. ANALYTICAL REPRESENTATION OF THE LOAD

The intensity of the transverse load is originally formulated in the following form

$$(2.1) \qquad q(\xi) = \frac{k}{2\tanh(k/2)} \frac{1}{\cosh^2\left[k\left(\xi - \frac{1}{2}\right)\right]} \frac{F}{L},$$

where k – dimensionless parameter $(0 < k < \infty)$, $\xi = x/L$ – dimensionless coordinate $(0 \leq \xi \leq 1)$, and the total transverse load

$$(2.2) \qquad F = L \int_0^1 q(\xi)\,\mathrm{d}\xi.$$

Consequently, the transverse shear force

$$(2.3) \qquad T(\xi) = -\frac{1}{2\tanh(k/2)} \tanh\left[k\left(\xi - \frac{1}{2}\right)\right] F,$$

and bending moment

$$(2.4) \qquad M_b\left(\xi\right) = \frac{1}{2k\tanh(k/2)} \ln \frac{\cosh(k/2)}{\cosh\left[k\left(\xi - \frac{1}{2}\right)\right]} FL.$$

The expressions (2.1), (2.3) and (2.4) comply with two basic relationships for beams: $q(x) = -\,\mathrm{d}T/drozx$, and $T(x) = \mathrm{d}M_b/\mathrm{d}x$. Generalized load of the beams includes the load types from uniformly distributed to concentrated force (three-point bending). The value of the dimensionless parameter k is decisive for the load type. Example diagrams of the intensity of the transverse load (2.1) for selected values of the parameter k and unitary load (2.2) ($F/L = 1$ N/m) are presented in Fig. 2.
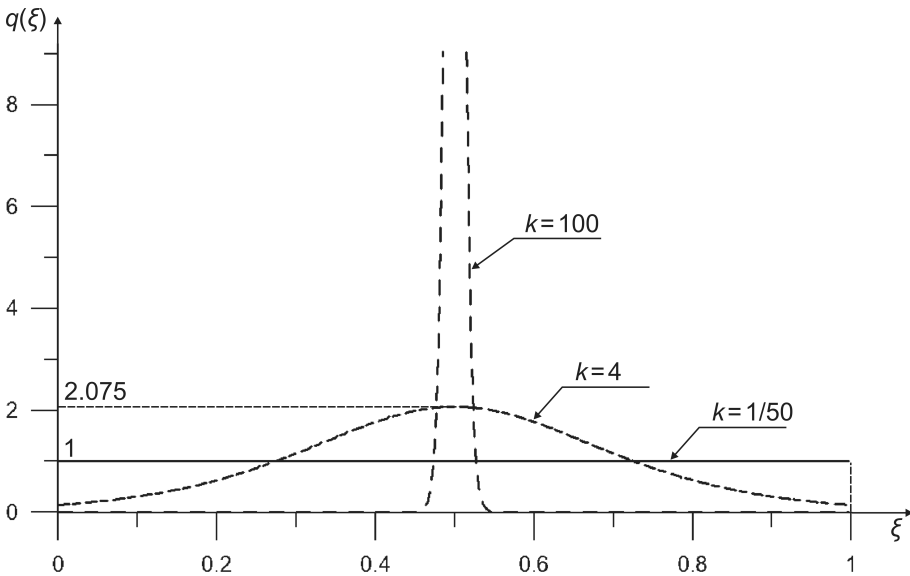
FIG. 2. Diagrams of the intensity of the transverse load (2.1).

Similarly, the diagrams of the shear force (2.3) for selected values of the parameter k and unitary force ($F = 1$ N) are presented in Fig. 3.

The diagrams of the bending moment (2.4) for selected values of the parameter k and unitary moment ($FL = 1$ N $\cdot$ m) are presented in Fig. 4.

It should be noticed that for growing values of the k parameter the plot becomes similar to the one characteristic for three-point bending, with its maximum approaching 0.25.

The mechanical properties of the beam symmetrically vary in the depth direction. The elasticity modules of the beam is formulated in the following form

$$(2.5) \qquad E(\eta) = E_1 f_e(\eta), \qquad G(\eta) = G_1 f_g(\eta),$$

where

$$f_e(\eta) = e_0 + (1 - e_0)\left(6\eta^2 - 32\eta^6\right)^{k_e}, \qquad f_g(\eta) = g_0 + (1 - g_0)\left(6\eta^2 - 32\eta^6\right)^{k_e},$$

$e_0 = \frac{E_0}{E_1}$, $g_0 = \frac{G_0}{G_1} = \frac{1+\nu_1}{1+\nu_0}e_0$, dimensionless parameters, E_j, G_j, ν_j – material constants ($j = 0$ for $\eta = 0$ and $j = 1$ for $\eta = \pm 1/2$), $\eta = \frac{y}{h}$ – dimensionless coordinate $\left(-\frac{1}{2} \leq \eta \leq \frac{1}{2}\right)$, k_e – exponent – natural number.
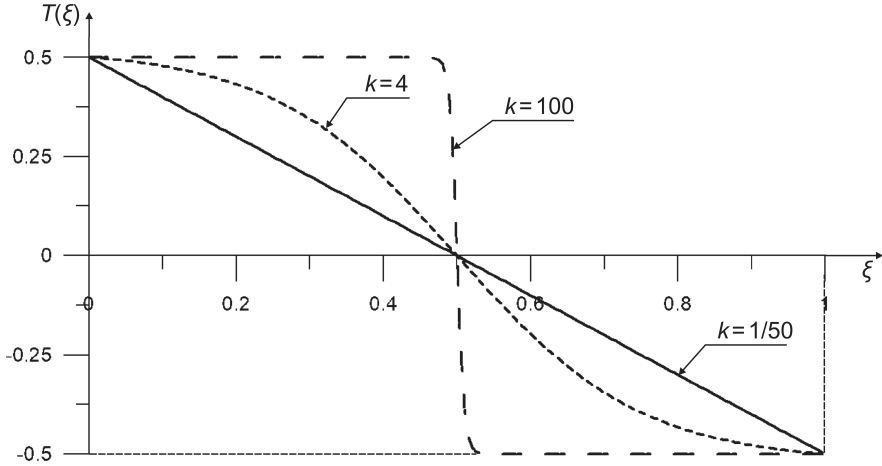
FIG. 3. Diagrams of the transverse shear force (2.3).
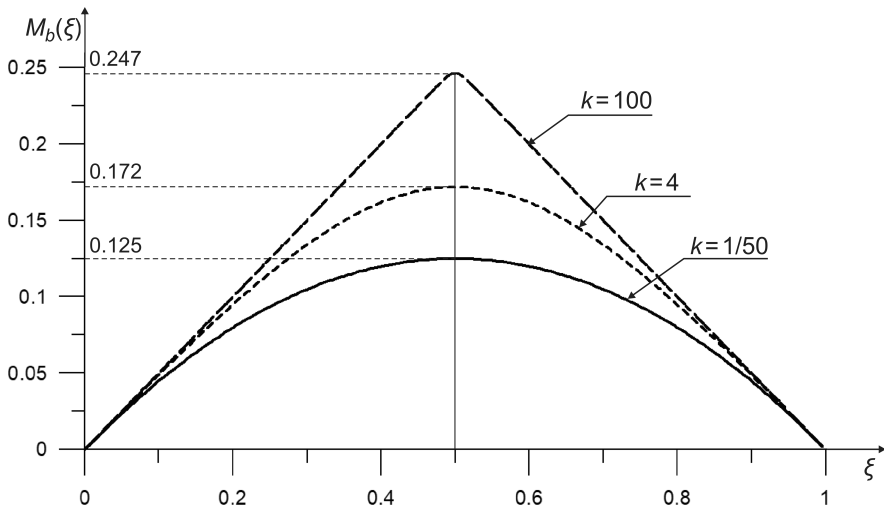
FIG. 4. Diagrams of the bending moment (2.4).

Variability of the elastic constants – Young's modules (2.5) in the depth direction of the beam is shown in Fig. 5.
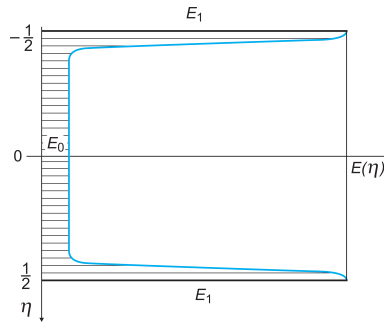
F<small>IG</small>. 5. Scheme of the variability of the Young's modules in the depth direction of the beam.

The objective of the study is calculation of the deflections of selected beams with consideration of the shear effect.

3. B<small>ENDING OF THE BEAM</small> – <small>ANALYTICAL STUDIES</small>

The nonlinear deformation of a planar cross section – the nonlinear "polynomial" hypothesis is assumed for purposes of analytical modeling of the beam. Scheme of the nonlinear deformation is shown in Fig. 6.
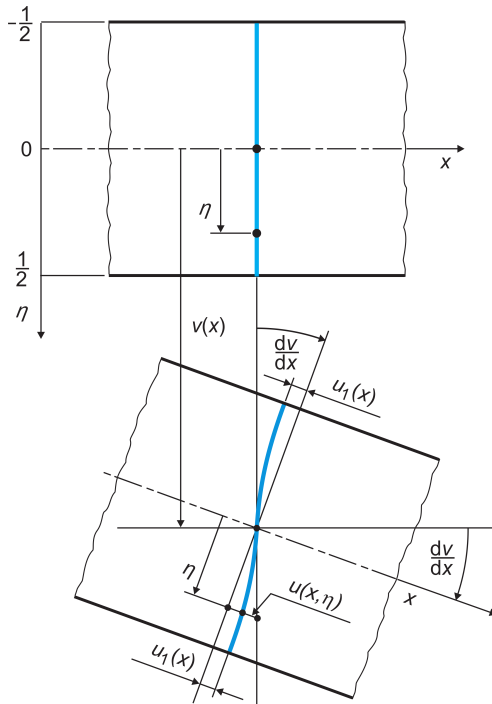
F<small>IG</small>. 6. Scheme of the nonlinear deformation of a planar cross section of the beam.

Taking into account the trigonometric nonlinear hypothesis formulated in [20] the longitudinal displacement of any cross section of the beam takes the following form

$$(3.1) \qquad u\left(x, \eta\right) = -h\left[\eta \frac{\mathrm{d}v}{\mathrm{d}x} - f_d(\eta)\psi(x)\right],$$

where polynomial function of the planar cross section deformation, analogic to the trigonometric one [20]

$$(3.2) \qquad f_d(\eta) = \frac{1}{1-\beta}\left[1 - \beta\left(3\eta - 4\eta^3\right)^{k_s}\right]\left(3\eta - 4\eta^3\right),$$

and $\psi(x) = \frac{u_1(x)}{h}$ – dimensionless function of the shear effect, $\beta = \frac{1}{1+k_s}$ – parameter, k_s – even exponent.

Therefore, the longitudinal and shear strains are as follows

$$(3.3) \qquad \varepsilon_x(x, \eta) = -h\left[\eta \frac{\mathrm{d}^2 v}{\mathrm{d}x^2} - f_d\left(\eta\right)\frac{\mathrm{d}\psi}{\mathrm{d}x}\right], \qquad \gamma_{xy}(x, \eta) = \frac{\mathrm{d}f_d}{\mathrm{d}\eta}\psi\left(x\right),$$

where $\frac{\mathrm{d}f_d}{\mathrm{d}\eta} = \frac{3}{1-\beta}\left[1 - \left(3\eta - 4\eta^3\right)^{k_s}\right]\left(1 - 4\eta^2\right)$ – the derivative of the function (3.2) with consideration of the relation $\beta = 1/(1 + k_s)$.

Consequently, the stresses in accordance with Hooke's law – expressions (2.5) and (3.3) are as follows

$$
\begin{aligned}
\sigma_x(x, \eta) &= -E_1 h\left[\eta \frac{\mathrm{d}^2 v}{\mathrm{d}x^2} - f_d\left(\eta\right)\frac{\mathrm{d}\psi}{\mathrm{d}x}\right] f_e\left(\eta\right), \\
(3.4) \\
\tau_{xy}(x, \eta) &= G_1 f_g\left(\eta\right)\frac{\mathrm{d}f_d}{\mathrm{d}\eta}\psi\left(x\right).
\end{aligned}
$$

Integration of the bending moment expression $M_b(x) = \displaystyle\int_A y\sigma_x\left(x, \eta\right)\mathrm{d}A$ provides the following differential equation

$$(3.5) \qquad C_{vv}\frac{\mathrm{d}^2 v}{\mathrm{d}x^2} - C_{v\psi}\frac{\mathrm{d}\psi}{\mathrm{d}x} = -\frac{M_b(x)}{E_1 b h^3},$$

where $C_{vv} = \displaystyle\int_{-1/2}^{1/2} \eta^2 f_e(\eta)\,\mathrm{d}\eta, \ C_{v\psi} = \displaystyle\int_{-1/2}^{1/2} \eta f_e(\eta)f_d(\eta)\,\mathrm{d}\eta$ – dimensionless coefficients.

Similarly, integration of the expression for transverse shear force $T(x) = \int_A \tau_{xy}(x,\eta)\,\mathrm{d}A$ gives

$$(3.6) \qquad \psi(x) = 2\frac{1+\nu_1}{C_\psi}\frac{T(x)}{E_1 bh},$$

where $C_\psi = \displaystyle\int_{-1/2}^{1/2} f_g(\eta)\frac{\mathrm{d}f_d}{\mathrm{d}\eta}\,\mathrm{d}\eta$ – dimensionless coefficient.

Taking into account the expression (2.3), the dimensionless function of the shear effect is in the following form

$$(3.7) \qquad \psi(\xi) = -\frac{1+\nu_1}{C_\psi}\frac{1}{\tanh(k/2)}\tanh\left[k\left(\xi-\frac{1}{2}\right)\right]\frac{F}{E_1 bh}.$$

Integrating the Eq. (3.5) with consideration of the expression (2.4) for bending moment, one obtains

$$(3.8)\quad C_{vv}\frac{\mathrm{d}v}{L\,\mathrm{d}\xi} = C_1 + C_{v\psi}\,\psi(\xi) - \frac{1}{2k\tanh(k/2)}\frac{F\lambda^2}{E_1 bh}\int \ln\frac{\cosh(k/2)}{\cosh\left[k\left(\xi-\frac{1}{2}\right)\right]}\,\mathrm{d}\xi,$$

where $\lambda = L/h$ – relative length of the beam, C_1 – integrating constant.

The angle of rotation $\mathrm{d}v/L\,\mathrm{d}\xi$ of the axis of the beam and the value of the function (3.7) at the beam middle ($\xi = 1/2$) are zero, therefore the integrating constant

$$(3.9) \qquad C_1 = \frac{J_1}{2k\tanh(k/2)}\frac{F\lambda^2}{E_1 bh},$$

where

$$J_1 = \int_0^{1/2} \ln\frac{\cosh(k/2)}{\cosh\left[k\left(\xi-\frac{1}{2}\right)\right]}\,\mathrm{d}\xi.$$

Integrating the Eq. (3.8) with consideration of the function (3.7), one obtains

$$(3.10) \qquad C_{vv}\widetilde{v}(\xi) = \frac{1}{2\tanh(k/2)}\left\{C_2 - \frac{1}{k}\left[f_s\left(\xi\right) - \lambda^2 f_b\left(\xi\right)\right]\right\}\frac{F}{E_1 bh},$$

where $\widetilde{v}(\xi) = v(\xi)/L$ – relative deflection of the beam,

$$f_s\left(\xi\right) = 2\left(1+\nu_1\right)\frac{C_{v\psi}}{C_\psi}\ln\left\{\cosh\left[k\left(\xi-\frac{1}{2}\right)\right]\right\},$$

$$f_b\left(\xi\right) = J_1\xi - \iint \ln\frac{\cosh(k/2)}{\cosh\left[k\left(\xi-\frac{1}{2}\right)\right]}\,\mathrm{d}\xi^2.$$

The deflection of the beam in the support point is zero $v(0) = 0$, therefore, the integrating constant

$$(3.11) \qquad C_2 = 2\left(1 + \nu_1\right) \frac{C_{v\psi}}{C_\psi} \frac{1}{k} \ln\left[\cosh\left(k/2\right)\right].$$

Thus, the maximal relative deflection of the beam based on the Eq. (3.10) for $\xi = 1/2$ is as follows

$$(3.12) \qquad \widetilde{v}_{\max}^{(\text{analyt})} = \max_{k_s}\left\{\widetilde{v}\left(\frac{1}{2}\right)\right\},$$

where

$$\widetilde{v}\left(\frac{1}{2}\right) = \frac{1}{2k \tanh\left(k/2\right)}\left[1 + k_{vs}\right] \frac{f_{vb}}{C_{vv}} \frac{F\lambda^2}{E_1 bh},$$

$$f_{vb} = \frac{1}{2}J_1 - \int\limits_0^{1/2}\!\!\int \ln \frac{\cosh\left(k/2\right)}{\cosh\left[k\left(\xi - \frac{1}{2}\right)\right]} \, \mathrm{d}\xi^2,$$

$$f_{vs} = 2\left(1 + \nu_1\right) \frac{C_{v\psi}}{C_\psi} \ln\left[\cosh\left(\frac{k}{2}\right)\right], \qquad k_{vs} = \frac{1}{\lambda^2} \frac{f_{vs}}{f_{vb}}$$

(k_{vs} – the shear coefficient for bending).

Value of the k_s parameter is calculated based on the expression (3.12), in accordance with [20].

Example calculations of the relative deflection $\widetilde{v}_{\max}^{(\text{analyt})}$ and the shear coefficient for bending k_{vs} are carried out for a beam family of selected sizes and material constants. The sizes of the cross section are $b = 50$ mm, $h = 60$ mm, material constants (SZYNISZEWSKI et al. [22]) $E_1 = 200$ GPa, $E_0 = 3150$ MPa, $\nu_1 = 0.3$, $\nu_0 = 0.05$, and the load-force $F = 5$ kN. The results of the calculations are specified in Tables 1–3. The calculated value of the exponent $k_s = 2$ (3.12).

Table 1. Values of maximal relative deflection of the beam and shear coefficient for uniformly distributed load ($k = 1/50$).

			λ			
			10	15	20	25
$k_e = 2$	$\widetilde{v}_{\max}^{(\text{analyt})}$		0.0002560	0.0005225	0.0008950	0.001374
	k_{vs}		0.202	0.0898	0.0505	0.0323
$k_e = 7$	$\widetilde{v}_{\max}^{(\text{analyt})}$		0.0004587	0.0008809	0.001472	0.002232
	k_{vs}		0.358	0.159	0.0895	0.0573
$k_e = 30$	$\widetilde{v}_{\max}^{(\text{analyt})}$		0.0007806	0.0015730	0.0026830	0.004110
	k_{vs}		0.231	0.103	0.0578	0.0370

Table 2. Values of maximal relative deflection of the beam and shear coefficient
for non-uniformly distributed load ($k = 4$).

		λ			
		10	15	20	25
$k_e = 2$	$\widetilde{v}_{\max}^{(\text{analyt})}$	0.0003377	0.0006858	0.001173	0.001800
	k_{vs}	0.212	0.0944	0.0531	0.0340
$k_e = 7$	$\widetilde{v}_{\max}^{(\text{analyt})}$	0.0006079	0.001160	0.001933	0.002927
	k_{vs}	0.376	0.167	0.0940	0.0602
$k_e = 30$	$\widetilde{v}_{\max}^{(\text{analyt})}$	0.001031	0.002067	0.003519	0.005384
	k_{vs}	0.243	0.108	0.0607	0.0388

Table 3. Values of maximal relative deflection of the beam and shear coefficient
for three-point bending ($k = 100$).

		λ			
		10	15	20	25
$k_e = 2$	$\widetilde{v}_{\max}^{(\text{analyt})}$	0.0004255	0.0008512	0.001447	0.002213
	k_{vs}	0.249	0.111	0.0623	0.0399
$k_e = 7$	$\widetilde{v}_{\max}^{(\text{analyt})}$	0.0007786	0.001454	0.002399	0.003615
	k_{vs}	0.441	0.196	0.110	0.0706
$k_e = 30$	$\widetilde{v}_{\max}^{(\text{analyt})}$	0.001303	0.002571	0.004345	0.006627
	k_{vs}	0.285	0.127	0.0712	0.0456

It should be noticed that, the shear effect k_{vs} in bending of the beams declines
with increasing length λ of the beam. The shapes of symmetrical variability of
the Young's modules (2.5) for selected values k_e assumed in the studies are shown
in Fig. 7.
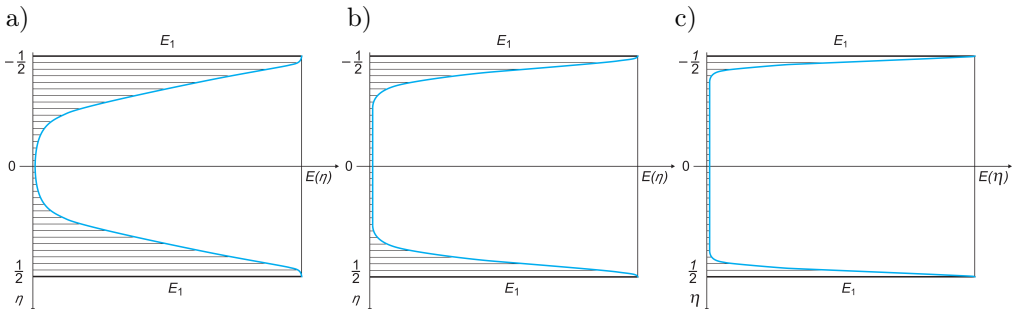
FIG. 7. Diagrams of variability of the Young's modules (2.5) for selected values k_e:
a) $k_e = 2$, b) $k_e = 7$, c) $k_e = 30$.

The shape of symmetrical variability of the Young's modules controlled by the value of the parameter k_e significantly affects the value of the shear effect k_{vs} in bending. This influence on the shear effect in bending is graphically presented in Fig. 8.
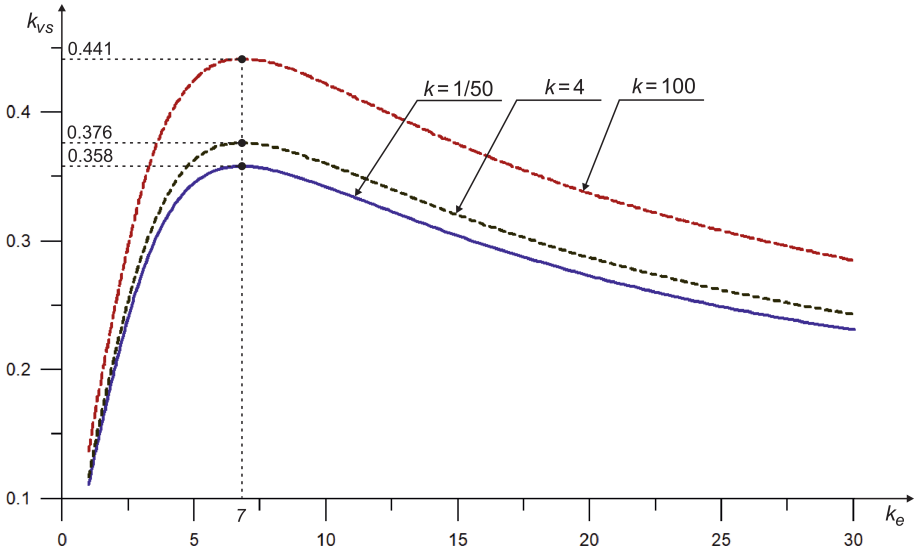
FIG. 8. Diagrams of the shear coefficient k_{vs} as a function of the exponent k_e ($\lambda = 10$).

The maximal value of the shear effect in bending of the beams with symmetrically varying mechanical properties occurs for the value of the exponent $k_e = 7$.

Particular case of the beam with symmetrically varying mechanical properties is the homogeneous beam. The mechanical properties (2.5) for this case are as follows: $E_1 = E$, $G_1 = G$, $\nu_0 = \nu_1 = \nu$, $e_0 = g_0 = 1$, $k_e = 0$. Moreover, the polynomial function of the planar cross section deformation (3.2) ($k_s = 0$) is in the following form

$$(3.13) \qquad f_d(\eta) = \left(3 - 4\eta^2\right)\eta.$$

Consequently, values of the dimensionless coefficients of the Eq. (3.5) are as follows: $C_{vv} = 1/12$, $C_{v\psi} = 1/5$ and $C_\psi = 2$. Therefore, the Eq. (3.5) is in the form

$$(3.14) \qquad \frac{\mathrm{d}^2 v}{\mathrm{d}x^2} - \frac{12}{5}\frac{\mathrm{d}\psi}{\mathrm{d}x} = -\frac{M_b(x)}{EJ_z},$$

where $J_z = bh^3/12$ – inertia moment of the cross section of the beam.

The dimensionless function of the shear effect (3.6) is as follows

$$(3.15) \qquad \psi(x) = (1+\nu)\frac{T(x)}{A},$$

where $A = bh$ – area of the cross section of the beam.

Thus, the maximal relative deflection of the beam with consideration of the expressions (2.3) and (2.4) is in the form

$$(3.16) \qquad \widetilde{v}_{\max}^{(\text{hom})} = \frac{6f_{vb}^{(\text{hom})}}{k\tanh(k/2)}\left[1 + k_{vs}^{(\text{hom})}\right]\frac{F\lambda^2}{Ebh},$$

where

$$f_{vb}^{(\text{hom})} = f_{vb} = \frac{1}{2}J_1 - \int\limits_0^{1/2}\int \ln\frac{\cosh(k/2)}{\cosh\left[k\left(\xi - \frac{1}{2}\right)\right]}\,\mathrm{d}\xi^2,$$

$$f_{vs}^{(\text{hom})} = \frac{1+\nu}{5}\ln\left[\cosh\left(\frac{k}{2}\right)\right],$$

$k_{vs}^{(\text{hom})} = \frac{1}{\lambda^2}\frac{f_{vs}^{(\text{hom})}}{f_{vb}^{(\text{hom})}}$ – the shear coefficient for bending.

Example calculations of the relative deflection $\widetilde{v}_{\max}^{(\text{hom})}$ and the shear coefficient for bending $k_{vs}^{(\text{hom})}$ are carried out for a beam family of selected sizes and material constants. The sizes of the cross section are $b = 50$ mm, $h = 60$ mm, material constants $E = 200$ GPa, $\nu = 0.3$, and the load-force $F = 5$ kN. The results of the calculations are specified in Table 4.

Table 4. Values of maximal relative deflection and shear coefficient of the homogeneous beam.

		λ			
		10	15	20	25
$k = 1/50$	$\widetilde{v}_{\max}^{(\text{analyt})}$	0.0001335	0.0002962	0.0005241	0.0008171
	k_{vs}	0.0250	0.0111	0.00624	0.00399
$k = 4$	$\widetilde{v}_{\max}^{(\text{analyt})}$	0.0001748	0.0003876	0.0006856	0.001069
	k_{vs}	0.0262	0.0117	0.00656	0.00420
$k = 100$	$\widetilde{v}_{\max}^{(\text{analyt})}$	0.0002146	0.0004749	0.0008394	0.001308
	k_{vs}	0.0308	0.0137	0.00770	0.00493

For the classical Euler-Bernoulli beam theory (without the shear effect), the relative deflection (3.16) is in the following form

$$(3.17) \qquad \widetilde{v}_{\max}^{(\text{hom})} = k_v^{(E-B)}\frac{FL^2}{EJ_z},$$

where

$$k_v^{(E-B)} = \frac{f_{vb}^{(\text{hom})}}{2k\tanh\left(k/2\right)}$$

is bending coefficient.

The values of this bending coefficient are $k_{v,1/50}^{(E-B)} = 0.013021 \approx 5/384$ for uniformly distributed load ($k = 1/50$) and $k_{v,100}^{(E-B)} = 0.02082 \approx 1/48$ for three-point bending ($k = 100$).

The proposed model of the beam subjected to generalized load with symmetrically varying mechanical properties and the hypothesis of planar cross section deformation enable to assess the shear effect arising while beam bending. The theory also includes the case of homogeneous beams.

4. Conclusions

The proposed generalized load controlled by the k parameter includes the whole range of the loads – from uniformly distributed to the concentrated one (three-point bending) – that is effective in studying bending of the beams.

Variation of the mechanical properties is controlled by k_e parameter (2.5). In case of $k_e = 0$ the structures is homogeneous, while for growing k_e the mechanical property pattern approaches the sandwich, i.e. three-layer structure. In case of the beam data adopted for the above example calculation the shear effect takes its maximum for $k_e = 7$ (Fig. 8).

The nonlinear "polynomial" hypothesis is controlled by the k_s parameter (Fig. 6). The k_s value is determined in result of maximization of the deflection (3.12).

In particular case of the beam model presented in the paper converts itself to the classical Euler-Bernoulli beam theory without the shear effect.

References

1. Wang C.M., Reddy J.N., Lee K.H., *Shear deformable beams and plates*, Elsevier, Amsterdam, Lausanne, New York, Shannon, Singapore, Tokyo, 2000.

2. Magnucki K., Stasiewicz P., *Elastic buckling of a porous beam*, Journal of Theoretical and Applied Mechanics, **42**: 859–868, 2004.

3. Magnucka-Blandzi E., *Axi-symmetrical deflection and buckling of circular porous-cellular plate*, Thin-Walled Structures, **46**: 333–337, 2008.

4. Thai H-T., Vo T.P., *Bending and free vibration of functionally graded beams using various higher-order shear deformation beam theories*, International Journal of Mechanical Sciences, **62**(1): 57–66, 2012.

5. Dehrouyeh-Semnani A.M., Bahrami A., *On size-dependent Timoshenko beam element based on modified couple stress theory*, International Journal of Engineering Science, **107**: 134–148, 2016.

6. Magnucki K., Malinowski M., Magnucka-Blandzi E., Lewiński J., *Three-point bending of a short beam with symmetrically varying mechanical properties*, Composite Structures, **179**: 552–557, 2017.

7. Paczos P., Wichniarek R., Magnucki K., *Three-point bending of the sandwich beam with special structures of the core*, Composite Structures, **201**: 676–682, 2018.

8. Sankar B.V., *An elasticity solution for functionally graded beams*, Composites Science and Technology, **61**: 689–696, 2001.

9. Kadoli R., Akhtar K., Ganesan N., *Static analysis of functionally graded beams using higher order shear deformation theory*, Applied Mathematical Modelling, **32**: 2509–2523, 2008.

10. Kapuria S., Bhattacharyyam M., Kumar A.N., *Bending and free vibration response of layered functionally graded beams: A theoretical model and its experimental validation*, Composite Structures, **82**: 390–402, 2008.

11. Giunta G., Belouettar S., Carrera E., *Analysis of FGM beams by means of classical and advanced theories*, Mechanics of Advanced Materials and Structures, **17**: 622–635, 2010.

12. Kahrobaiyan M.H., Rahaeifard M., Tajalli S.A., Ahmadian M.T., *A strain gradient functionally graded Euler-Bernoulli beam formulation*, International Journal of Engineering Science, **52**: 65–76, 2012.

13. Li S-R., Cao D-F., Wan Z-Q., *Bending solutions of FGM Timoshenko beams from those of the homogenous Euler-Bernoulli beams*, Applied Mathematical Modelling, **37**: 7077–7085, 2013.

14. Zhang D-G., *Nonlinear bending analysis of FGM beams based on physical neutral surface and high order shear deformation theory*, Composite Structures, **100**(3): 121–126, 2013.

15. Rahaeifard M., Kahrobaiyan M.H., Ahmadian M.T., Firoozbakhsh K., *Strain gradient formulation of functionally graded nonlinear beams*, International Journal of Engineering Science, **65**: 49–63, 2013.

16. Chen D., Yang J., Kitipornchai S., *Elastic buckling and static bending of shear deformable functionally graded porous beam*, Composite Structures, **133**: 54–61, 2015.

17. Li L., Hu Y., *Nonlinear bending and free vibration analyses of nonlocal strain gradient beams made of functionally graded material*, International Journal of Engineering Science, **107**: 77–97, 2016.

18. Nejad M.Z., Hadi A., *Eringen's non-local elasticity theory for bending analysis of bidirectional functionally graded Euler-Bernoulli nano-beams*, International Journal of Engineering Science, **106**: 1–9, 2016.

19. Sayyad A.S., Ghugal Y.M., *Bending, buckling and free vibration of laminated composite and sandwich beams: A critical review of literature*, Composite Structures, **171**: 486–504, 2017.

20. Magnucki K., Witkowski D., Lewinski J., *Bending and free vibrations of porous beams with symmetrically varying mechanical properties – Shear effect*, Mechanics of Advanced Materials and Structures (published online: 16 May 2018).

21. TAATI E., *On buckling and post-buckling behavior of functionally graded micro-beams in thermal environment*, International Journal of Engineering Science, **128**: 63–78, 2018.

22. SZYNISZEWSKI S.T., SMITH B.H., HAJJAR J.F., SCHAFER B.W., ARWADE S.R., *The mechanical properties and modelling of a sintered hollow sphere steel foam*, Materials & Design, **54**: 1083–1094, 2014.